

DESIGN OF POST-TENSIONED TIMBER BEAMS FOR FIRE RESISTANCE

**Phillip M. Spellman, Anthony K. Abu, David M. Carradine, Peter J. Moss, and
Andrew H. Buchanan**

Department of Civil and Natural Resources Engineering, University of Canterbury, Private Bag
4800, Christchurch 8140, New Zealand

e-mails: pms128@uclive.ac.nz, tony.abu@canterbury.ac.nz, david.carradine@canterbury.ac.nz,
peter.moss@canterbury.ac.nz, andy.buchanan@canterbury.ac.nz

Keywords: Post-Tensioned Timber, Fire Performance, Furnace Test, Design

Abstract. *This paper describes a series of three full-scale furnace tests on post-tensioned LVL box beams loaded with vertical loads, and presents a proposed fire design method for post-tensioned timber members. The design method is adapted from the calculation methods given in Eurocode 5 and NZS:3603 which includes the effects of changing geometry and several failure mechanisms specific to post-tensioned timber. The design procedures include an estimation of the heating of the tendons within the timber cavities, and relaxation of post-tensioning forces. Additionally, comparisons of the designs and assumptions used in the proposed fire design method and the results of the full-scale furnace tests are made. The experimental investigation and development of a design method have shown several areas which need to be addressed. It is important to calculate shear stresses in the timber section, as shear is much more likely to govern compared to solid timber. The investigation has shown that whilst tensile failures are less likely to govern the fire design of post-tensioned timber members, due to the axial compression of the post-tensioning, tensile stresses must still be calculated due to the changing centroid of the members as the fire progresses. Research has also highlighted the importance of monitoring additional deflections and moments caused by the high level of axial loads.*

1 INTRODUCTION

Timber is the material of choice for residential construction in New Zealand, Australia and many parts of the world, however commercial and industrial construction are dominated by steel and concrete. Post-tensioned timber is a building technique designed to offer a timber solution for multi-storey industrial and commercial buildings with long spans and open floor plans serving as an alternative to steel and concrete. There are many benefits in using post-tensioned timber over steel and concrete in that buildings can be constructed very quickly with substantially smaller lifting equipment, timber is an easy material to work with, and timber is also a green and sustainable building material which is becoming increasingly important when making decisions about building materials for larger buildings [1-3].

Post-tensioned (PT) timber construction is an adaptation of the mature technology of post-tensioned pre-stressed concrete. PT timber is made with large timber cross sections, constructed from engineered timber products such as glue laminated timber (Glulam) or laminated veneer lumber (LVL). Timber box-beams are post-tensioned with un-bonded high strength steel bars or wire tendons which run through cavities within members, fixed to steel anchorages at either end of the beams or frames [4]. The post-tensioning can be run through multiple bays of a frame to form the primary moment resisting beam-column connections as demonstrated in Figure 1.

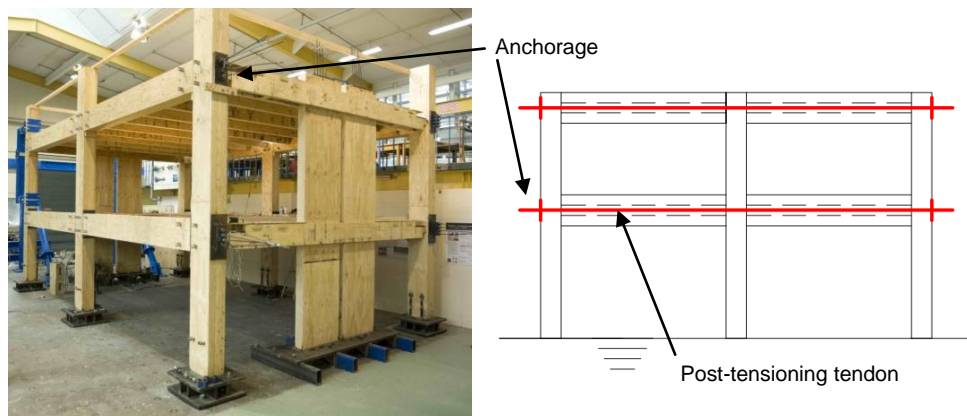


Figure 1: Left - 2/3rd scale post-tensioned timber frame used for seismic testing. Right - Multiple beam-column connections made with post-tensioning. (Thicker lines represent the steel tendons and anchorages).

Post-tensioning can be used to reduce deflections of heavy timber beams. The tendons can be draped to provide uplift at mid-span. In seismic designs the post-tensioning serves to re-centre the building following an earthquake, eliminating residual displacement. Energy dissipation can be achieved with easily replaceable mild steel energy dissipaters.[5-8]

As with any timber construction there is a commonly perceived increased risk in fire. While the fire performance of heavy timber structures is well established, PT timber has a number of factors which could lead to unique and unfavourable failure mechanisms in fire. Complications include cavities within timber members and the use of high strength steel tendons. As a result, corner rounding due to charring may have a greater influence on a PT timber member compared to a timber member with no cavity. A small rise in tendon temperature may result in substantial relaxation of the post-tensioning force, potentially causing premature loss of connections or the failure of a member.

In order to demonstrate the fire performance of post-tensioned timber members a series of 3 full-scale furnace tests on post-tensioned timber members were completed. These tests also provide data for the validation of the fire design method developed for post-tensioned timber members. The design method provides advice on the analysis of post-tensioned timber members under fire conditions, and the failure mechanisms which are important to consider.

2 FULL-SCALE FURNACE TESTS

The experimental testing took place utilising a 4m by 3m furnace at the Wellington based Building Research Association of New Zealand (BRANZ) testing facility. The beams were designated A, B and C, and were LVL box beams, each post-tensioned with two 7-wire strand (12.7mm diameter) tendons. Beam A was 426mm by 300mm, Beam B was 236mm by 190mm, and Beam C was 300mm by 190mm. Each beam was constructed from 63mm thick LVL having a published bending stiffness of 13 GPa. Beams A and B had approximately 210kN of post tensioning applied and Beam C had 230 kN post tensioning applied. Beam B failure prematurely with an unexpected failure mechanism which lead to revisions in the design calculations and eventually the construction and testing of Beam C. Because of this, no all the data for Beam B is not presented here. Further details of this series of tests is available in [9].

2.1 Failure times

The failure times for the three tests are given in Table 1, together with the failure mechanisms and the char depth.

Table 1: Char depths and failure times and mechanisms from the full-scale test series.

Beam	Char depth	Failure time	Failure mechanism
A	48mm	64 min	Shear in lower corner
B	18mm	22 min	Premature disconnection of top flange
C	40mm	56 min	Bending and compression at end of beam and beneath loading point.

2.2 Displacements

During the Beam A test the deflections remained in the order of 0.5mm-1mm for the first 45 minutes then started to increase steadily until approximately 64 minutes when the beam became unable to carry the applied load. The deflection profile during the Beam C test was similar to the Beam A test, however, due to the beam being more flexible due to its geometry, deflections were greater. The deflections measured during each test are presented in Figure 2 (left).

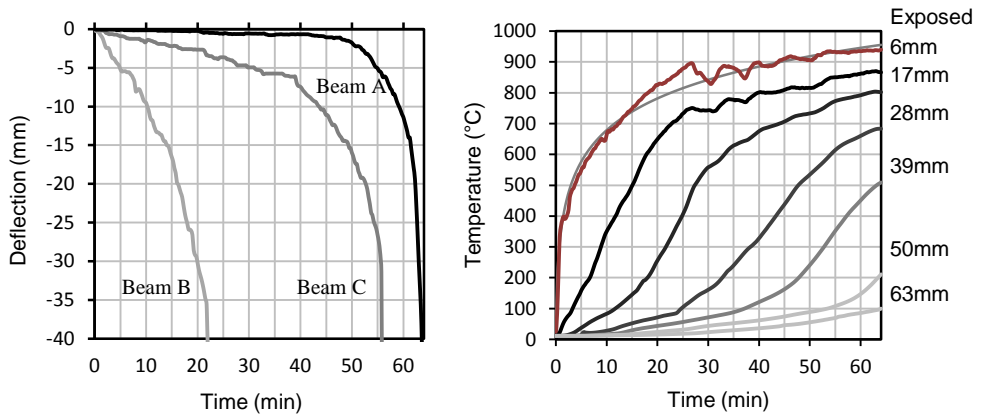


Figure 2: (left) Vertical deflections of the test beams during standard fire exposure; (right) Thermal profile through the bottom flange of Beam A.

2.3 Thermal results

The temperature profiles of each beam did not vary significantly, therefore only the behaviour of a single beam is presented. During exposure to the ISO834 fire, the temperature profiles close to the surface followed the random variations in the furnace temperature. Further into the section these features became less evident and the curves became comparatively smoother. Deeper than 17mm into the section, the temperatures approached 100 °C slowly and once 100°C was reached, heated more quickly. The bottom flanges heated slightly more quickly than the webs since the flanges shields the web from some of the furnace heat and therefore receive more radiation. Another possibility is that the width of the beam is small enough that the 2-dimensional heat transfer serves to increase the temperature more quickly. The temperature distribution for Beam A is presented in Figure 2 (right).

The temperature of the inside face of the LVL did not appreciably rise beyond 100°C whilst the beams were still intact. The tendon temperature lagged behind the internal timber surface temperature as expected. After 45 minutes the internal timber surface was approximately 25-30 °C hotter than the tendons within Beam A. The temperature of the internal surface and the tendon are presented in Figure 3 (left). The position of the tendon within the cavity in Beam A showed little effect on tendon temperature. The temperature profiles for the tendon at various positions are presented in Figure 3 (right).

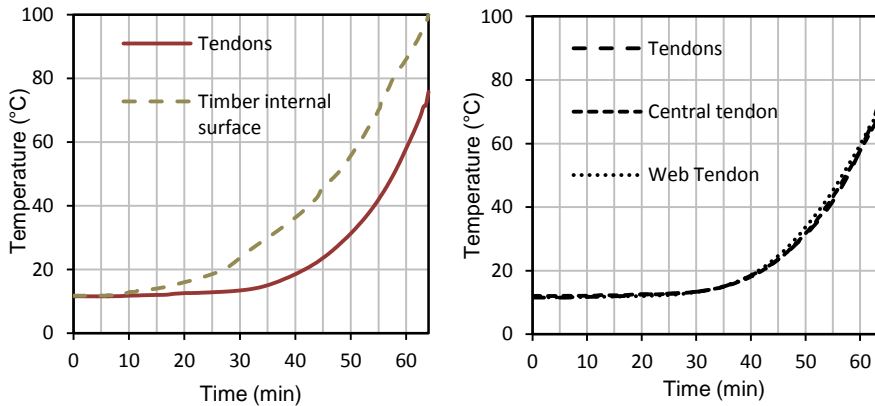


Figure 3: (Left) Average temperature of the post-tensioning tendon and the internal surface of the timber cavity of beam A; (right) Temperature profiles tendons at different positions in cavity.

2.4 Tendon post-tension force and relaxation

Over the course of each test the post-tensioning forces decreased with time. The causes of these decreases were due to the heating of the tendons and their subsequent thermal expansion and loss of stiffness, but also the loss of timber cross section, and rotation of end anchorages. During the Beam A test, at 60 minutes the tendons had lost approximately 25% of the initial applied stress. At this time the tendon temperatures were approximately 58°C.

3 FIRE DESIGN METHOD

3.1 Failure mechanisms

Under fire conditions it is important to check: combined bending and compression at mid span and at the end of beams, as well as shear in the lower corners and webs. The shear in lower corners needs to be considered due to the geometry of the beams; charring rounds the exposed corners leading to the thinnest region of the beam occurring there. These failure modes can be considered using standard methods such as a combined stress index for bending and compression and ensuring adequate strength in shear.

3.2 Section Shape during fire exposure

LVL has a char rate of 0.72mm/min, as published by the manufacturer. The corners of a timber section exposed to fire round as they char. This can be modelled by assuming the corner radius is equal to the char depth [10]. These assumptions can be used to estimate the section geometry over the fire duration. Shown in Figure 4 is a visual comparison between the geometry constructed from the above assumptions and a similar timber section which has been exposed to fire. The section geometry can be made up from a series of simple geometric shapes, which can then be used to calculate the second moment of area (I), cross-sectional area ($A_{Timber,Fire}$), centroid location, and therefore tendon eccentricity (e_{fire}).

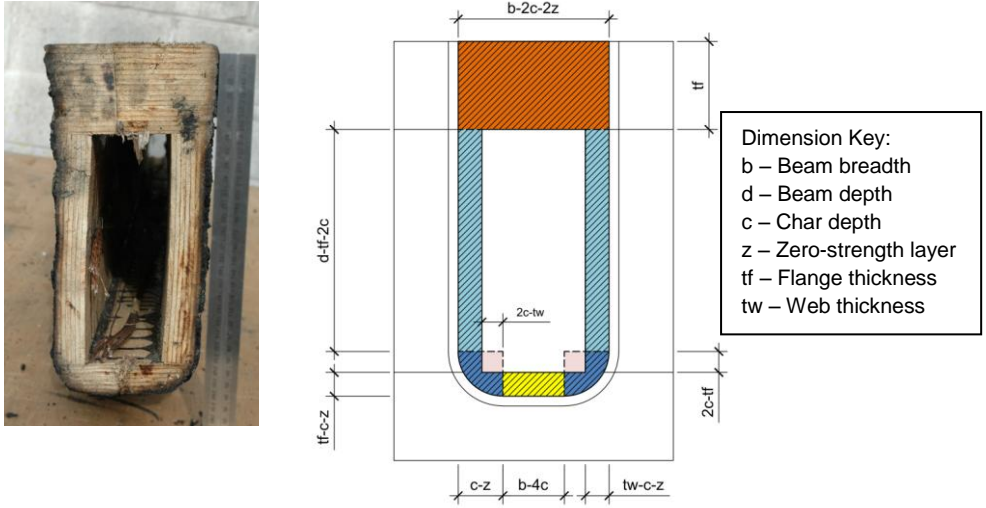


Figure 4: Comparison between an actual fire exposed timber section and the model geometry. (Note: pink coloured areas are removed for sectional analyses.)

3.3 Deflection and post tensioning relaxation analysis

When heated, the post-tensioning loses tensile load due to thermal expansion of the steel and a reduction of Young's Modulus with increased temperature. There are additional changes to the force within the tendons due to anchorage rotations, beam deflections, and the increase in compressive stresses due to the loss of area resulting in shortening of the beam. These geometry effects can be included in the analysis as effective strains. The strains in the tendon can be represented as shown in Equation (1) **Error! Reference source not found.**, where: $\epsilon_{0,mech}$ is the total mechanical strain of the tendon at ambient conditions, $\epsilon_{mechanical}$ is the axial strain due to the applied axial force, $\epsilon_{thermal}$ is the thermal strain, $\epsilon_{rotation}$ is the effective strain due to the rotation of the anchorages and subsequent elongation of the tendons final length, and $\epsilon_{compression}$ is the effective strain due to the increased axial deflections of the timber beam.

$$\epsilon_{0,mech} + \epsilon_{rotation} + \epsilon_{compression} = \epsilon_{mechanical} + \epsilon_{thermal} \quad (1)$$

As the calculation of deflections and post-tensioning force are non-linear and depend on one another, the calculation lends itself to being solved iteratively.

In-order to calculate the components of strain within the tendon it is important to calculate the initial length of the tendon so that each strain component is calculated with the same reference length. The initial length of the tendon can be calculated as shown in Equation (2), where, E_{Tendon} is the Modulus of Elasticity of the tendon, A_{Tendon} is the cross sectional area of the tendons, L is the length of the beam, and F_{PT} is the ambient initial post tensioning force applied to the tendons.

$$L_o = \frac{E_{Tendon} A_{Tendon} L}{F_{PT} + E_{Tendon} A_{Tendon}} \quad (2)$$

3.3.1 Post-tensioning force

The goal of this calculation is to determine the reduced post-tensioning force in the tendons after a specified fire duration. However, due to the iterative nature of this calculation it is required that an initial

value is assumed. It is easiest to assume the ambient temperature post-tensioning force as this initial value as it will allow the calculation to converge quickly.

3.3.2 Post-tensioning moment

The applied post-tensioning moment is determined from the post-tensioning force and the calculated eccentricity. It is important to include the effect of the changing eccentricity due to the changing cross section geometry.

3.3.3 Transverse loading

The external loads are determined as dictated by the fire limit state loading and will not change between iterations. The Australia and New Zealand Structural design actions standard AS/NZS:1170 [11] states that the fire limit state load case to be the dead load plus 40% of the live load.

3.3.4 Tendon temperature

The temperature of the tendon can be assumed to be the same temperature as the internal surface of the cavity within the timber member. This is a conservative assumption as the tendons will take additional time to heat. The internal timber temperature and therefore the tendon temperature can be estimated using an assumed temperature distribution for the timber underneath the char layer. Structural design for fire safety [12] presents the parabolic distribution presented in Equation (3) where: $T(x)$ is the temperature of the timber at a distance x beneath the char layer, T_i is the initial or ambient temperature of the timber (20°C), T_p is the charring or pyrolysis temperature of the timber (300°C), a is the thickness of the heat-affected layer (40mm).

$$T(x) = T_i + (T_p - T_i) \left(1 - \frac{x}{a}\right)^2 \quad (3)$$

3.3.5 Thermal strain

The thermal strain in the tendon can then be estimated using the relationship presented in Section 3.4 of Eurocode 2 which provides the thermal strain for a pre-stressing steel [13]. This calculation is intended for use with pre-stressed concrete and since the tendons being used for post-tensioned timber are the same as those used for pre-stressed concrete, it is appropriate to use this calculation. Equation (4) presents the thermal strain relationship adapted from Eurocode 2 where $\varepsilon_{thermal}$ the strain is induced in the tendon due to its temperature, and θ is the temperature of the tendon in °C.

$$\varepsilon_{thermal} = -2.016E^{-4} + 10^{-5}\theta + 0.4 \times 10^{-8}\theta^2 \quad (4)$$

3.3.6 Beam deflections

Under fire conditions it is important to consider the deflections of a post-tensioned timber beam so that the bowing moment induced by the axial loads can be included in the calculation. The deflection components which need to be monitored during design are flexural deflection due to external loads (D_{Load}), shear deflection (D_{Shear}) due to external loads, flexural deflections due to the post-tensioning moment (D_{PT}), and bowing deflection caused by the axial post-tensioning force acting on an initially deflected member (D_{Bowing}). The moment and deflections due to axial loads are dependent on the total deflection, which includes a component of its own deflection making this a non-linear problem. Equation (5) presents components of deflection and Equation (6) presents the calculation of the bowing deflection.

$$D_{Total} = D_{Load} + D_{PT} + D_{Shear} + D_{Bowing} \quad (5)$$

$$D_{Bowing} = \frac{F_{PT} D_{Total} L^2}{\pi^2 E_{Timber} I} \quad (6)$$

3.3.7 Beam end rotations

Rotation at end anchorages affects the forces developed in tendons. This occurs under both ambient and fire conditions. The beam end rotation components (φ_{end} , Equation (7)) to consider include the end rotation due to transverse loading (φ_{Load}), post-tensioning (φ_{PT}), and axial bowing ($\varphi_{Bowling}$ Equation (8)). Tendon elongation due to rotation at the anchorages can be converted to strain using Equation (9) which depends on the initial tendon length (L_o) as a reference and the tendon eccentricity (e_{Fire}).

$$\varphi_{end} = \varphi_{Load} + \varphi_{PT} + \varphi_{Bowling} \quad (7)$$

$$\varphi_{Bowling} = \frac{F_{PT,Fire} D_{total} L}{\pi E_{Timber} I} \left(-\cos\left(\frac{\pi L}{4}\right) + 1 \right) \quad (8)$$

$$\varepsilon_{rotation} = \frac{2\varphi_{end} e_{Fire}}{L_o} \quad (9)$$

3.3.8 Additional timber compression

As the timber is post-tensioned there are large axial loads which compress the timber resulting in deflections parallel to the longitudinal axis of the beams. This is implicitly taken into account during stressing, however, during fire exposure the timber area resisting the axial load is reduced which increases the stress developed in the cross section and therefore increases compression deflections. It is only the change in compressive strain which is of interest during this calculation which can be calculated using Equation (10).

$$\varepsilon_{compression} = \frac{F_{PT,fire} L}{L_o E_{timber} A_{Timber,fire}} - \frac{F_{PT} L}{L_o E_{timber} A_{Timber}} \quad (10)$$

3.3.9 Tendon strain

The mechanical strain, which is used to calculate the force within the tendon, can then be calculated using Equation (11).

$$\varepsilon_{mechanical} = \varepsilon_{0,mech} + \varepsilon_{rotation} + \varepsilon_{compression} - \varepsilon_{thermal} \quad (11)$$

3.3.10 Stiffness reduction

As a tendon is heated, Young's modulus decreases. Eurocode 2 section 3.2.4 [13] provides a relationship between the reduction of Young's modulus and tendon temperature.

3.3.11 Post-tensioning tendon force

The reduced tendon force for each iteration can then be calculated with Equation (12). Where E_{fire} is the temperature reduced young's modulus of the post tensioning tendon.

$$F_{PT,Fire}^{i+1} = \varepsilon_{mechanical} E_{fire} A_{tendon} \quad (12)$$

3.4 Design Actions

The mid-span bending action can be calculated with Equation (13): where $M_{Bowling}^*$ is the moment due to axial loads as calculated in Equation (14), M_{PT}^* is the moment due to post-tensioning and $M_{Load,Fire}^*$ is the moment due to loading. The end moment due solely to post-tensioning, as all other components are zero at the ends of beams. The axial action on beams should be the reduced post-tensioning force. The shear flow action should be calculated for the web at the centroid and at the bottom corners of beams. Stresses can then be combined in an appropriate manner and checked against strength capacities in order to design adequately performing members.

$$M_{Total,Fire}^* = M_{Bowling}^* + M_{PT}^* + M_{Load,Fire}^* \quad (13)$$

$$M_{Bowling}^* = F_{PT,Fire} D_{Total} \quad (14)$$

4 DISCUSSION

The char rate recommendation of this research is 0.72mm/min with an additional 7mm layer. Using this recommended char rate provides the best correlation between the fullscale test failure times and those predicted by the proposed design method. The predicted char depths and failure times for the three beams tested are shown in Table 2

Table 2: Predicted failure times using a 0.72mm/min char rate and 7mm zero strength layer.

Beam	Predicted Char depth	Predicted Failure time	Measured Char depth	Measured Failure time
A	47.5 mm	61 min	48mm	64 min
B	33.5 mm	37 min	18mm	22 min
C	45 mm	53 min	40mm	56 min

The hand calculation method of estimating the temperature of the inner surface of the timber has been shown to provide reasonable results, and is able to be used to estimate tendon temperatures conservatively. The hand calculation method gives results slightly cooler than those observed on the timber surface but approximately 10°C higher than the tendon temperatures recorded anywhere in the cavity. The recorded temperatures of the timber cavity surface and the tendons within beam C and those predicted with the hand calculation method are compared in Figure 5.

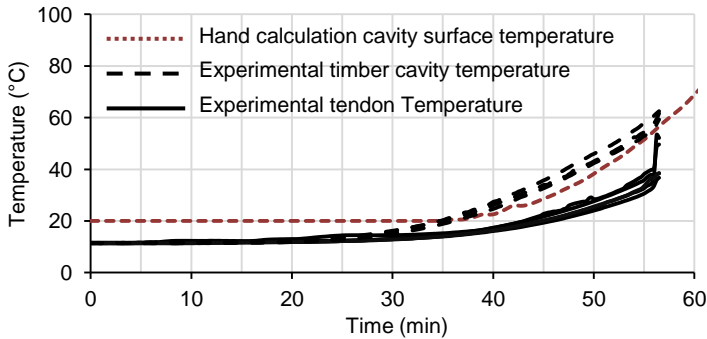


Figure 5: Tendon temperatures estimated by hand calculations and as recorded during full scale testing of Beam C.

4.1 Tendon relaxation

The simplified calculation method provides a reasonable estimate of the relaxation of the post tensioning tendons. Figure 6 shows the calculated tendon strength for Beams A and B compared to the full-scale experimental results. It was found that the tendon force is significantly better modelled by including the effects of tendon elongation or shortening due to end rotations and increased timber compression as well as the loss of stiffness and increased thermal strain. Rotation of the anchorages increases strain in the tendons. Compression stresses and strains in the timber due to axial post-tensioning increase during a fire due to the reduction in timber cross-section. Before including these effects, the relaxation calculation depended only on the thermal strain and reduction of Young's modulus and greatly over predicted the remaining force in the post-tensioning

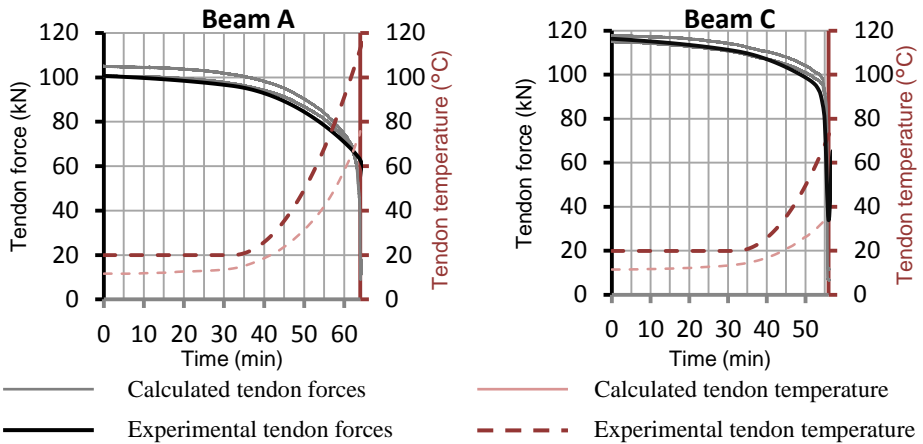


Figure 6: Simplified calculation method tendon relaxation for Beam A (left) and Beam C (right) compared with experimental results

4.2 Deflections

Deflections calculated by the hand calculation method substantially under-predict the beams deflections. Figure 7 shows the calculated deflections for both beams compared to the experimental deflections recorded. Experimental deflections were measured at the loading points and mid-span deflections were therefore slightly larger than shown. The calculated deflections for Beam A were positive due to the post-tensioning moment overcoming the loading and causing the beam to deflect upwards. The calculated deflections for Beam C follow the shape of the recorded deflections better than Beam A, but still substantially under predict deflections. Due to the non-linear nature of the deflection calculation, it can become numerically unstable and fail to reach a solution. This however should not occur before the calculation method predicts failure. The inability of the calculation method to predict deflections, casts doubt on the rest of the calculation which depends on the deflections, particularly the post-tensioning relaxation, and the design actions. A possible source of error in this calculation is the assumption for the elasticity of the timber. Timber plasticity or thermally accelerated creep may account for the increased downwards deflections observed during testing

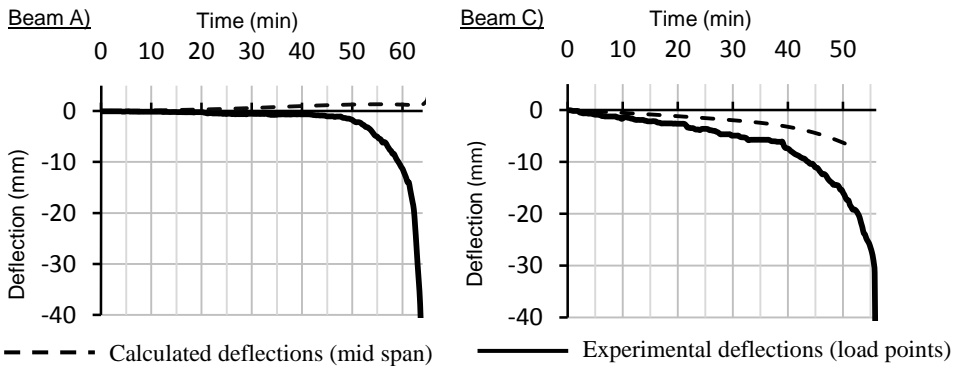


Figure 7: Calculated and experimental beam deflections

5 CONCLUSIONS

A series of full-scale fire tests were conducted on loaded post-tensioned timber beams and a design method has been proposed. The design method includes the following failure mechanisms which need to be considered during the fire design of post-tensioned timber beams:

- Shear failure in the webs at the centroid,
- Shear failure in bottom corners,
- Bending and compression failure at mid-span,
- Bending and compression failure at the ends of the beam

The proposed design method is able to predict the fire resistance of a post-tensioned timber beam and the tendon relaxation reasonably accurately. The design method recommends a char rate of 0.72mm/min and an additional 7mm zero strength layer. The design method does not yet capture the beam deflections at failure, possibly due to the lack of a model for plasticity of wood at elevated temperatures, which needs further investigation.

REFERENCES

- [1] John, S.: Environmental Impacts of Multi-Storey Buildings Using Different Construction Materials. 2008, MAF
- [2] John, S., N. Perez, and A.H. Buchanan: The Carbon Footprint of Multi-storey Timber Buildings Compared with Conventional Materials WCTE 2010, in *11th World Conference on Timber Engineering*. 2010: Riva del Garda, Trentino, Italy.
- [3] Smith, T.J.: Feasibility of Multi Storey Post-Tensioned Timber Buildings: Detailing, Cost and Construction., in *Department of Civil and Natural Resources Engineering*. 2008, University of Canterbury: Christchurch, New Zealand. p. 155.
- [4] Buchanan, A., A. Palermo, and D. Carradine: Post-Tensioned Timber Frame Buildings. *The Structural Engineer*, 2011. 89: p. 17.
- [5] Beerschoten, W.V., A. Palermo, D. Carradine, F. Sarti, et al.: Experimental Investigation on the Stiffness of Beam- Column Connections in Post Tensioned Timber Frames, in *Structural Engineers World Congress 2011*. 2011: Italy.
- [6] Iqbal, A., S. Pampanin, A. Palermo, and A.H. Buchanan: Seismic performance of full-scale post-tensioned timber beam-column joints in *The 11th World Conference of Timber Engineering*. 2010: Riva del Garda, Trentino Italy.
- [7] Newcombe, M.: Design Procedures and Numerical Analysis for Multistorey Post-Tensioned Timber Buildings (Not Yet Published). 2010, University of Canterbury, New Zealand.
- [8] Newcombe, M.: Seismic Design of Multistorey Post-Tensioned Timber Buildings. 2007, University of Pavia: Pavia.
- [9] Spellman, P., D. Carradine, A. Abu, P. Moss, et al.: Full-scale fire tests of post-tensioned timber beams, in *To be published in the 12th World Conference on Timber Engineering proceedings*. 2012: Auckland, New Zealand.
- [10] Buchanan, A.: Timber Design Guide. Third Edition ed. 2007, Wellington: New Zealand Timber Industry Federation Inc.
- [11] Standards New Zealand: AS/NZS 1170:2002 Structural design actions. 2002.
- [12] Buchanan, A.: Structural design for fire safety. 2001: Wiley Chichester, UK.
- [13] British Standard Institute: Eurocode 2: Design of concrete structures - part 1-2: General rules - Structural fire design. 2004: U.K.